Published in final edited form as:
Hepatology. 2009 November ; 50(5): 1512–1523. doi:10.1002/hep.23186.

Inhibition of Phosphatidylinositol 3-Kinase Signaling in Hepatic Stellate Cells Blocks the Progression of Hepatic Fibrosis

Gakuhei Son[1], **Ian N. Hines**[1], **Jeff Lindquist**[1], **Laura W. Schrum**[2], and **Richard A. Rippe**[1]

[1]Division of Gastroenterology and Hepatology, Department of Medicine, University of North Carolina, Chapel Hill, North Carolina

[2]Department of Biology, University of North Carolina, Charlotte, North Carolina

Abstract

The hepatic stellate cell (HSC) is the primary cell type in the liver responsible for excess collagen deposition during fibrosis. Following a fibrogenic stimulus, the cell changes from a quiescent vitamin A storing cell to an activated cell type associated with increased extracellular matrix synthesis and increased cell proliferation. The phosphatidylinositol 3-kinase (PI3K) signaling pathway has been shown to regulate several aspects of HSC activation *in vitro*, including collagen synthesis and cell proliferation. Using a targeted approach to inhibit PI3K signaling specifically in HSCs, we investigated the role of PI3K in HSCs using a rodent model of hepatic fibrosis. An adenovirus expressing a dominant negative form of PI3K under control of the smooth muscle α-actin (αSMA) promoter was generated (Ad-SMAdnPI3K). Transducing HSCs with Ad-SMAdnPI3K resulted in decreased proliferation, migration, collagen expression, and several additional profibrogenic genes, while also promoting cell death. Inhibition of PI3K signaling was also associated with reduced activation of Akt, $p70^{S6K}$, and extracellular regulated kinase (ERK) signaling as well as reduced cyclin D1 expression. Administering Ad-SMAdnPI3K to mice following bile duct ligation resulted in reduced HSC activation and decreased extracellular matrix deposition, including collagen expression. A reduction in profibrogenic mediators, including tumor growth factor – β (TGF-β), tissue inhibitor of metalloproteinase – 1 (TIMP-1), and connective tissue growth factor (CTGF) was also noted. However, liver damage, assessed by alanine aminotransferase (ALT) levels, was not reduced.

Conclusion—Inhibition of PI3K signaling in HSCs during active fibrogenesis inhibits extracellular matrix (ECM) deposition, including synthesis of type I collagen, and reduces expression of profibrogenic factors. These data suggest that targeting PI3K signaling in HSCs may represent an effective therapeutic target for hepatic fibrosis.

Keywords

bile duct ligation; growth factor; collagen; liver cirrhosis; intracellular cell signaling

Introduction

Liver fibrosis represents a wound healing process in response to a variety of acute and chronic stimuli, including ethanol, viral infections, cholestasis, and metabolic diseases (1,2). Characterized by excess synthesis and deposition of extracellular matrix (ECM), fibrosis disrupts the normal architecture of the liver leading to organ dysfunction, which can

Correspondence: Richard A. Rippe, Ph.D., CB #7032, Medical Biomolecular Research Building; Room 7340B, Division of Gastroenterology and Hepatology, Department of Medicine, University of North Carolina, Chapel Hill, Chapel Hill, NC 27599-7032, Tel. 919 966-7469; Fax. 919 966-7468, rarippe@med.unc.edu.

progress to cirrhosis and ultimately organ failure if left untreated. Currently, few therapeutic strategies exist to treat liver fibrosis.

The hepatic stellate cell (HSC) is primarily responsible for excess deposition of extracellular matrix proteins (ECM) during fibrosis. Following a fibrogenic stimulus, HSCs lose their retinoid stores, proliferate, express smooth muscle α-actin (αSMA), and produce large amounts of extracellular matrix proteins, including type I collagen. Phosphatidylinositol 3-kinase (PI3K) is a key signaling molecule composed of an 85-kDa regulatory subunit and a 110-kDa catalytic subunit which is recruited to and activated by the activated PDGF receptor following HSC activation and growth factor stimulation (3). The importance of PI3K signaling in HSCs has been established as blocking PI3K activity, using either pharmacological (LY294002) or genetic approaches, inhibits HSC proliferation and collagen gene expression, a process involving interruption of key downstream signaling pathways, including Akt and $P70^{S6K}$ (4,5). Activation of Akt is associated with HSC proliferation and α1(I) collagen transcription and translation (4,6–8). Likewise, interruption of the $p70^{S6K}$/mTOR signaling suppresses HSC proliferation. Therefore, interruption of PI3K signaling is capable of suppressing key components of HSC activation and proliferation and may represent a therapeutic target for treating hepatic fibrosis.

Since αSMA expression is induced following HSC activation, we developed an αSMA driven expression vector to direct expression of a dominant negative form of PI3K to prevent HSC proliferation and collagen expression in activated HSCs. We demonstrate that inhibition of PI3K signaling *in vivo*, specifically in HSCs, dramatically attenuates experimentally induced hepatic fibrosis in mice.

Materials and Methods

Adenovirus Preparation

The dnPI3K coding sequence was amplified from Ad-dnPI3K (9) using PCR with a forward primer 5′-gatcatgatc*ggatcc*ccacc**atgtacccatacgatgttccaga**-3′, containing the HA-tag (bold), and a reverse primer 5′-gatcatgatc*ggatcc*tcatcgcctctgctgcgcgt-3′. The amplified product was digested with *Bam* HI and cloned into the *Bam* HI site in the pDNR plasmid (BD Bioscience, San Jose, CA). The insert was sequenced to assess the orientation of the insert and the correct sequence. The αSMA promoter was amplified from the pSMP8 plasmid (10) using forward primer 5′-gatcatgatc*gaattc*acaccataaaacaagtgcatgag-3′ and reverse primer 5′-gatcatgatc*gaattc*agctgcaccagcgtctcagg-3′ and the PCR product cloned into the pTOPO plasmid (Invitrogen, Calsbad, CA). The αSMA promoter was excised from the pTOPO plasmid using *Eco* RI and cloned into the *Eco* RI site in dnPI3K-pDNR upstream of the dnPI3K insert. Sequencing confirmed orientation and integrity of the insert. The recombinant adenovirus was generated using the BD Adeno-x Expression System Promoterless Vector (BD Bioscience, San Jose, CA) according to the manufacturers' protocol. HSCs transduced with the recombinant adenovirus expressed the HA-tag, as assessed by Western blot analysis. Hepatocytes, endothelial cells, and Kupffer cells did not express the HA-tag when transduced by Ad-SMAdnPI3K, thus confirming cell specific expression (data not shown).

Hepatic Stellate Cell Isolation

Mouse HSCs were isolated as previously described (11,12) from pCOL9GFP-HS4,5 transgenic mice (collagen promoter-driven GFP transgenic mice) on a BALB/c background which have been described previously (13). Isolated HSCs were cultured in DMEM supplemented with 10% FBS in a 95% air − 5% CO_2 atmosphere. Hepatocyte, endothelial cell, and Kupffer cell isolation procedures are provided in supplementary materials. All

animal procedures were performed under the guidelines set by the University of North Carolina Institutional Animal Care and Use Committee and are in accordance with those set by the National Institute of Health.

GFP Quantification

HSCs from pCol9GFP-HS4,5 mice were plated in 6-well plates (2×10^5 cells/well). After 5 days, cells were transduced with Ad-SMAdnPI3K, Ad-βgal, or no virus. After 12 hr, the medium was changed to media containing 10% FBS. After 48 hr, plates were scanned for GFP expression and quantified by phosphorimager analysis according to the recommend protocol of the manufacturer (GE Healthcare, Piscataway, NJ).

Fibrosis Model

pCol9GFP-HS4,5 transgenic mice on a BALB/c background were subjected to double ligation of the common bile duct (BDL) (14). Sham-treated animals underwent the same procedure without ligation. Some mice were administered carbon tetrachloride (CCl_4) to induce fibrosis with specific procedures provided in supplementary materials. All procedures were in accordance and approved by the Institutional Animal Care and Use Committee guidelines at the University of North Carolina at Chapel Hill. Ad-SMAdnPI3K, 1×10^9 PFU, was administered 4 days following BDL via tail vein injection. Mice were sacrificed 9 or 18 days after BDL, and blood and liver samples were harvested.

Assessment of Apoptosis

In vitro, cell death was determined by propidium iodide (PI, Sigma, St. Louis, MO) and Hoechst 33342 (Sigma, St. Louis, MO) double fluorescent staining. HSCs were isolated from pCol9GFP-HS4,5 transgenic mice and cultured in 6-well plates. After 5 days in culture, HSCs were transduced with Ad-SMAdnPI3K, Ad-βgal, no virus, as above. After 24 hr, the cells were incubated with Hoechst (1 μg/ml) and PI (5 μg/ml) for 20 min. Afterwards, cells were visualized by fluorescent microscopy. Paraffin embedded liver sections were stained for DNA fragmentation using the *In Situ* Cell Death Detection Kit, TMR red (Roche, Indianapolis, Indiana) according to the manufacturers' recommendations.

Histological Analysis and Immunohistochemistry

Portions of the liver were collected at the time of sacrifice and fixed in 10% buffered formalin for 24 hr at 4°C. Expression of αSMA was determined in paraffin-embedded sections by immunohistochemistry as previously described (15). For fibrosis, liver sections were stained with Picrosirius Red (Sigma, St. Louis, MO) as previously described (15). For immunofluorescent staining, liver specimens were fixed using 4% paraformaldehyde for 16 hr at 4° C, incubated in PBS containing 30% sucrose 24 hr, then frozen at −80°C in OCT Compound (Sakura Finetek USA, Inc. Torrance, CA). Sections were incubated with monoclonal antibody to HA (1:100; Cell Signaling, Danvers, MA) using the MOM kit (Vector Laboratories, Burlingame, CA) and Alexa Fluor 546 Streptavidin (Invitrogen) used for visualization. Hepatic GFP expression was assessed using frozen tissue sections and viewed by fluorescent microscopy. For triple staining, PFA fixed frozen sections were stained with anti-GFP (chicken polyclonal; Aves Labs, Inc), anti-HA (mouse monoclonal), and anti-Desmin (rabbit polyclonal; Thermo Scientific) all at a dilution of 1:100. For visualization, goat anti-chicken conjugated to FITC (to stain GFP), goat-anti-rabbit conjugated to AlexaFluor 350 (to stain Desmin), and goat anti-mouse conjugated to AlexaFluor 546 (to visualize HA) were incubated on the sections for 30 minutes at room temperature. For immunofluorescence cell staining, 24 hr after Ad-SMAdnPI3K transduction (MOI: 300), HSCs were fixed with 4% paraformaldehyde and −20°C methanol (10 min, room temperature). The cells were then incubated with anti-HA antibody 1:100

using the MOM Kit. Sirius red-positive area, αSMA-positive area, and GFP-positive area were quantified using Image J software (NIH Image; http://rsb.info.nih.gov/ij/) from 5 random non-overlapping 100× fields for each animal with 6 animals assessed in each group.

Antibodies

Protein extracts were prepared from liver tissue (50 μg) or cultured HSCs (20 μg) using RIPA buffer and separated on 8–16% Tris-glycine gels and transferred to PVDF membranes as previously described (16). Antibodies against phospho-PI3K (Tyr^{458}), PI3K, phospho-Akt^{Ser473}, Akt, phospho-$p70^{S6K}$(Thr^{421}/Ser^{424}), $p70^{S6K}$, phospho-Erk (Thr^{202}/Tyr^{204}), Erk, Cyclin D1, CD31, HA-Tag (1:1000; all from Cell Signaling), αSMA (1:5000; Sigma), albumin (1:5000; ICN), F4/80 (1:1000; Serotec), and β-Actin (1:1000; Sigma) were used for western blot procedures. incubated overnight at 4°C in Tris-buffered saline containing 0.05% Tween-20 (TTBS) and 5% nonfat dry milk. Appropriate horseradish peroxidase conjugated secondary antibodies diluted 1:2,000–5,000 in TTBS + 5% nonfat dry milk were then incubated with blots for 1 hr at room temperature. Antibody staining was visualized by enhanced chemiluminescence (ECL plus, Amersham, Indianapolis, IN) exposed to film. Band density was quantified from digital images using Image J software.

Other methods

Procedures for cell isolation, proliferation, and migration, hydroxyproline and alanine aminotransferase assay, western blotting, and RT-PCR are provided in supplementary materials.

Statistical analysis

All data are presented as means ± SEM (standard error of the mean). Differences between Ad-SMAdnPI3K group and control groups were assessed by unpaired Student's *t*-test. *P*-values <0.05 were considered statistically significant.

Results

Inhibition of PI3K signaling reduces cell proliferation and migration in isolated HSCs

To determine the role of PI3K signaling in HSCs *in vivo*, we constructed an adenovirus that allows for HSC specific expression of a dominant negative form of PI3K (9) using the αSMA promoter (10). This recombinant adenovirus expressed the HA-tag in HSCs, but not in hepatocytes, Kupffer cells, or endothelial cells (Figure 1A). In isolated HSCs, αSMA expression was first detected following 2 days in culture (data not shown). We, therefore, transduced isolated HSCs with Ad-SMAdnPI3K at Day 2 and noted weak expression of the HA-tag one day after viral transduction, which progressively increased by 5 days in culture (data not shown). Therefore, for our *in vitro* studies, we transduced HSCs after 4 days in culture to assure high levels of expression of HA-dnPI3K from the αSMA promoter.

Previous studies have shown that PI3K positively regulates rat HSC proliferation (4). To confirm that similar effects occur in murine HSCs, mouse HSCs were isolated and cultured for 4 days. Cells were left untreated or transduced with Ad-βgal or Ad-SMAdnPI3K in serum free media for 48 hours. Cell proliferation was stimulated using media containing 10% FCS and cells monitored for 72 hr. Control cells, or cells transduced with Ad-βgal, showed similar increases in growth rate during the experimental time period; however, cells transduced with Ad-SMAdnPI3K showed a significant reduction in cell numbers, compared to Ad-βgal transduced cells (Figure 1B).

To determine whether PI3K signaling influences HSC migration, a wound assay was performed and the distance cells migrated from the wound was assessed following a 24 hr

culture period. Control HSCs or cells transduced with Ad-βgal showed similar migratory responses; however, cells transduced with Ad-SMAdnPI3K showed a significant reduction in cell migration, compared to control Ad-βgal transduced cells (Figure 1C).

Inhibition of PI3K decreases expression of α1(I) collagen in HSCs mediated in part by inhibiting gene transcription

We first examined the expression pattern of the HA-tag present on dnPI3K and GFP, a marker for collagen expression, in HSCs from pCol9GFP-HS4,5 transgenic mice transduced with Ad-SMA-dnPI3K. Some cells expressed only GFP, other cells only expressed the HA-tag; however, only a few cells expressed both the HA-tag and GFP (Figure 1D). This result is similar to that previously reported where HSCs express either αSMA or collagen, with only a few cells expressing both genes (10).

To confirm that blocking PI3K also inhibits α1(I) collagen gene expression in murine HSCs, similar to that shown in rat HSCs (4), we examined the effect of Ad-SMAdnPI3K on collagen expression in HSCs from pCol9GFP-HS4,5 transgenic mice. HSCs were either left untreated or transduced with Ad-βgal or Ad-SMAdnPI3K after 5 days in culture. A significant reduction in GFP fluorescence, a marker for collagen expression in these cells, was observed following viral transduction with Ad-SMAdnPI3K (Figures 1E); a similar reduction in α1(I) collagen mRNA expression was also observed (Figure 1F). Therefore, blocking PI3K activity in HSCs inhibits α1(I) collagen gene expression, at least partially at the transcriptional level.

Inhibiting PI3K induces cell death in murine HSCs

Since HSC proliferation was reduced when PI3K activity was blocked (Figure 1B), we examined whether this inhibition is associated with increased cell death. HSCs were isolated and cultured for 5 days, then transduced with Ad-βgal or Ad-SMAdnPI3K. Transduction with Ad-SMAdnPI3K markedly increased propidium iodide staining, compared to cells transduced with Ad-βgal (Figure 2 A–F). Therefore, inhibition of PI3K activity in activated HSCs promoted membrane permeability and nuclear envelope disruption, processes associated with cell death.

Expression of genes associated with a fibrogenic response is reduced in HSCs following inhibition of PI3K signaling

Since inhibiting PI3K activity reduced collagen gene expression in HSCs, we examined the effect of PI3K inhibition on the expression of several other pro-fibrogenic genes. HSCs were cultured for 5 days, then either left untreated or transduced with Ad-SMAdnPI3K or Ad-βgal. After 48 hr, mRNA expression of TGF-β, αSMA, TIMP-1, CTGF were significantly reduced in cells transduced with Ad-SMAdnPI3K, compared to Ad-βgal transduced cells (Figure 2G). In contrast, expression of PPARγ was increased 2.3-fold (Figure 2G). These findings correlate with a reduced fibrogenic response of the activated HSC when PI3K signaling is interrupted.

Inhibition of PI3K signaling in activated HSCs blocks activation of Akt and $p70^{S6K}$ signaling and cyclin D1 expression

To examine a potential mechanism by which inhibition of PI3K signaling may mediate an anti-fibrogenic response, we assessed the effects of blocking PI3K on ERK, PI3K, Akt, and $p70^{S6K}$ signaling pathways, known to influence the fibrogenic response in HSCs. Day 5 HSCs were transduced with Ad-βgal or Ad-SMAdnPI3K, serum starved for 24 hours, then stimulated with 10% serum and activation of PI3K and MAPK signaling analyzed. Increased phosphorylation of the PI3K p85 subunit was observed after 30 min in both PBS and Ad-

βgal treated cells (Figure 3A). In contrast, phosphorylation of PI3K, Akt, and $p70^{S6K}$ was completely blocked in cells transduced with Ad-SMAdnPI3K, but not in PBS treated or Ad-βgal transduced cells. Phosphorylation of Erk was only modestly attenuated by Ad-SMAdnPI3K (Figure 3A).

To investigate a potential mechanism for reduced HSC proliferation when PI3K signaling is blocked, we examined the influence of PI3K signaling on cyclin D1 expression, previously shown to regulate HSC proliferation (17,18). Isolated HSCs were cultured for 5 days, transduced with Ad-βgal or Ad-SMAdnPI3K, then serum starved for 48 hr. Cells were then stimulated to proliferate using 10% serum for 24 hours and cyclin D1 gene expression assessed. Control cells and cells transduced with Ad-βgal showed increased cyclin D1 expression over the 24 hr time period (Figure 3B). In contrast, cells transduced with Ad-SMAdnPI3K failed to induce cyclin D1 expression (Figure 3B), thus demonstrating that PI3K induces cyclin D1 expression in activated HSCs, which is partially responsible for inducing HSC proliferation in activated HSCs.

Expression of αSMA driven dnPI3K in experimentally induced hepatic fibrosis

To examine cell specific expression of Ad-SMAdnPI3K during experimentally induced liver fibrosis, pCol9GFP-HS4,5 transgenic mice underwent BDL and 4 days later were administered PBS or 1×10^9 PFU of either Ad-βgal or Ad-SMAdnPI3K. Two days following adenovirus administration expression of HA was detected in liver extracts from mice administered Ad-SMAdnPI3K, while no HA expression was detected in the PBS or Ad-βgal treated animals (Figure 4A). BDL induced significant GFP expression in both PBS and Ad-βgal treated mice; however, mice administered Ad-SMAdnPI3K showed a marked attenuation of GFP fluorescence, indicative of reduced collagen gene expression (Figure 4B). Interestingly, GFP expression did not appreciably co-localize to expression of the HA tag expressed by Ad-SMAdnPI3K. A discordant expression of collagen expression and αSMA expression in activated HSCs has previously been reported (10). Since expression of dnPI3K in cultured HSCs induced cell death (Figure 2A–F), we examined if HSC death was induced in the Ad-SMAdnPI3K treated animals. Indeed, HSC death was increased, assessed by TUNEL staining, in the animals in which Ad-SMAdnPI3K was administered, but not in PBS or Ad-βgal treated animals (Figure 4C). To further assess the co-localization *in vivo* of the adenovirus within HSCs, triple staining for GFP, the marker of collagen expression, desmin, a marker of hepatic stellate cells, and HA, a marker of virus expression was performed on day 6, two days following adenoviral administration. As shown in Figure 4D, there is appreciable co-localization of desmin, collagen-GFP, and HA at this time point following adenoviral administration. Given the effects of PI3K inhibition of HSC survival both *in vitro* and *in vivo*, we chose to also look at co-localization of HA and GFP at an earlier time-point hypothesizing that HSC death had already occurred 4 days following adenovirus administration. Provided in Supplemental Figure 1, co-localization of HA and GFP could be observed 1 day following adenovirus administration (Day 5 post-BDL). Together, these data demonstrate the ability of dnPI3K driven by the αSMA promoter to be expressed in stellate cells *in vivo* and induce their apoptosis within the cholestatic liver.

Inhibiting PI3K signaling attenuates hepatic αSMA expression in BDL-induced liver fibrosis

To determine the extent of activated HSCs in the liver following BDL-induced liver fibrosis, immunohistochemical analysis for αSMA expression, a classical marker of activated HSCs, was performed. Induction of liver fibrosis resulted in an increase in αSMA expression in the livers of animals treated with either PBS or Ad-βgal 9 and 18 days following BDL, respectively (Figures 5A, 5B). Both significant interstitial and vascular αSMA expression was observed. αSMA expression was attenuated in the Ad-SMAdnPI3K treated animals

where the interstitial expression pattern was mostly resolved, but vascular expression remained relatively high (Figures 5A, 5B). Western blot analysis confirmed the immunohistochemical staining (Figure 5C).

Inhibition of PI3K signaling attenuates collagen expression and deposition following BDL

Given the profound impact of PI3K inhibition on HSC αSMA expression *in vivo* following BDL, expression of collagen was examined. As shown in Figure 6A–B, Sirius red staining was significantly reduced in Ad-SMAdnPI3K treated mice subjected to BDL for 9 or 18 days when compared to control treated or Ad-β-gal treated mice subjected to BDL. Moreover, tissue hydroxyproline levels were significantly reduced following 18 days of BDL in AD-SMAdnPI3K when compared to control or β-gal treated mice subjected to BDL (Figure 6C). GFP expression was significantly reduced as was steady-state α1(I) collagen mRNA expression following either 9 or 18 days of BDL, compared to control treated or Ad-β-gal treated mice subjected to BDL (Figure 6D–F). Consistent with its effects in the BDL model of liver fibrosis, administration of Ad-SMAdnPI3K reduced fibrogenesis in the carbon tetrachloride model of liver injury and fibrosis to a similar degree (Supplemental Figure 2). Interestingly, a dnPI3K driven by the CMV promoter, and thus expressed in all cells, led to significant reduction in collagen gene expression (Supplemental Figure 3) in conjunction with significant morbidity in animals in both models of liver fibrosis, a process which could be correlated with significant reduction in functional liver mass. These data demonstrate the ability of PI3K to support fibrogenesis and highlight important cell specific functions of this signaling protein. Additional studies are underway to understand the importance of PI3K in other cell types, including hepatocytes within the chronically damaged liver.

Ad-SMAdnPI3K inhibits hepatic expression of fibrogenic genes during BDL-induced liver fibrosis, but does not reduce liver injury

To assess the effect of Ad-SMAdnPI3K on expression of other genes associated with liver fibrosis, we examined the expression of TGF-β, αSMA, TIMP-1, and CTGF in the livers of animals from each experimental group. Following 9 days of BDL, expression of TGF-β, αSMA, TIMP-1, and CTGF were all increased and all were significantly reduced in animals administered Ad-SMAdnPI3K, but not in control animals (Figure 7A). Liver injury was also increased in the livers of the experimental animals; however, despite a reduction in the progression of fibrosis, ALT levels were not reduced following administration of Ad-SMAdnPI3K (Figure 7B).

Discussion

Liver fibrosis is a key risk factor for the development of cirrhosis and chronic liver failure. Activation of hepatic stellate cells (HSCs) is a crucial component of this process (1,2). Here, we show the importance of PI3K signaling in the development and progression of hepatic fibrogenesis *in vivo* and during HSC activation, proliferation, and pro-fibrogenic collagen production *in vitro*. In doing so, a HSC specific adenoviral vector was created which directed strong selectivity for expression in activated, smooth muscle actin positive, HSCs.

Phosphatidylinositol 3-kinase (PI3K) represents a key signaling molecule that controls many cellular functions, such as proliferation, survival, adhesion, and migration (3,4). In the liver, macrophage-associated PI3K activation promotes cytokine production and subsequent hepatocyte proliferation early following partial hepatectomy (19). Hepatocyte-associated PI3K regulates growth following a reduction in liver volume, a process involving Akt activation. In the setting of fibrosis, PI3K is activated via PDGF receptor ligation following carbon tetrachloride treatment and correlates with collagen production (20). In the present

study, inhibition of PI3K activity, via a dominant negative form of PI3K within HSCs, reduced hepatic fibrogenesis following BDL. Inhibition of fibrogenesis was associated with reduced TGFβ expression, αSMA expression, and collagen production. Several mechanism(s) may exist by which PI3K might promote this activation. First, PI3K induced Akt activation leads to cell survival and proliferation. Sustained activation of Akt has been shown to induce significant cellular proliferation, likely involving $p70^{S6K}$ activation and increased cyclin D1 expression (4). This is consistent with the present study showing that inhibition of PI3K in HSCs *in vitro* decreased cyclin D1 expression and reduced cellular proliferation. Lending to the connectivity of this pathway, inhibition of PI3K in HSCs inhibited $p70^{S6K}$ activation. Previous studies have shown that inhibition of the mTOR/$p70^{S6K}$ pathway by rapamycin in HSCs reduces G1 to S phase progression (17). Therefore, inhibiting PI3K, and thus its downstream signaling mediators, significantly impacts cell growth and proliferation (21–23).

In addition to reduced proliferation, impairment of PI3K activity in HSCs was associated with the induction of cell death. Interruption of PI3K activity in HSCs led to a substantial increase in TUNEL staining *in vivo* and membrane permeability *in vitro*, suggesting the induction of cell death rather than a transition back to quiescence. The mechanism(s) promoting this response are not clear, though inhibition of MAPK pathways, specifically Erk, could be partially responsible. Erk activation is associated with suppression of caspase induction and mitochondrial permeability changes (24). Moreover, Akt activation suppresses Bad function, a pro-apoptotic factor (25). Indeed, it has been postulated that clearance of activated HSCs is a critical step in fibrosis resolution within the liver and, from data presented here, PI3K inhibition may represent a novel mechanism for their elimination.

A third mechanism by which PI3K may function to promote the fibrogenic response is through the regulation of pro-fibrogenic mediator production by HSCs. Interruption of PI3K activity suppressed TGFβ and PDGF expression by HSCs *in vitro* and hepatic expression of these factors during cholestasis and their production of these factors likely promotes autocrine activation. Moreover, PI3K activation may suppress PPARγ expression. Previous studies have demonstrated the importance of PPARγ in suppressing hepatic fibrogenesis *in vivo* and HSC activation *in vitro* (26). *In vitro*, PPARγ expression is reduced as HSCs become activated and its overexpression leads to suppression of collagen production and αSMA expression, a process involving inhibition of p300 transactivation (27–29). In our study, restoration of PPARγ function could be one mechanism by which PI3K inhibition leads to suppression of collagen production and HSC activation. In sum, interruption of PI3K activity is capable of influencing multiple cellular levels, from cell survival and proliferation to the promotion of growth factor production, to drive hepatic fibrogenesis.

Another interesting finding in the present study was the observed heterogeneity of HSCs both *in vitro* and *in vivo*. Previous studies by Magness *et al*. identified cells within the damaged liver which expressed either αSMA, collagen, or both suggesting the potential for either multiple cell populations with characteristics similar to HSCs (10). In the setting of BDL, it is clear that extrahepatic myofibroblasts are recruited periportally and contribute significantly to hepatic fibrogenesis, in the absence of significant αSMA expression (30). For *in vitro* studies, however, HSCs are enriched from undamaged livers. Similar to the *in vivo* studies in the BDL model, HSCs express either αSMA or collagen or both. Thus, the use of αSMA driven dnPI3K may only function in a subset of the collagen producing cells within the liver. Alternatively, when PI3K activity is blocked in HSCs, cell death is induced (Figure 2A–F). Nevertheless, our approach has led to a large and significant reduction in collagen expression and deposition, and inhibition of pro-fibrogenic growth factor production, both *in vitro* and *in vivo*. The overall significance of multiple HSC populations, or intermediates within this lineage, remains to be determined.

In summary, we have demonstrated that selective inhibition of PI3K in activated HSCs, via a αSMA-driven dominant negative form of PI3K, reduces hepatic fibrogenesis, likely through suppression of fibrotic gene transcription, as well as through promotion of HSC death. *In vitro* studies further demonstrate the ability of PI3K inhibition to suppress HSC proliferation, migration, and pro-fibrogenic gene expression, processes which likely involves interruption of downstream signaling molecules including Akt and $p70^{S6K}$. Furthermore, this inhibition appears to be critical for the induction of HSC death, thereby eliminating important collagen producing cells from the liver. In addition, the current investigation has also revealed, as previous studies would indicate, a potential heterogeneity of collagen producing cells within the liver, specifically the presence of αSMA-negative collagen producing cells. Finally, the current study has led to the creation and validation of an activated HSC specific adenoviral vector which will provide a platform for future investigation into the functions of other cellular proteins within HSCs, both *in vitro* and *in vivo*. In conclusion, PI3K is critical for HSC activation and collagen production and, as such, therapies directed at inhibiting PI3K, specifically in HSCs, may be useful to treat hepatic fibrogenesis.

Supplementary Material

Refer to Web version on PubMed Central for supplementary material.

Acknowledgments

Financial Support: Supported by NIH Grants DK065972 (RAR) and AA016563 (INH).

Abbreviations

HSC	hepatic stellate cells
PI3K	phosphatidylinositol 3-kinase
αSMA	smooth muscle α-actin
$p70^{S6K}$	p70 S6 Kinase
ERK	extracellular regulated kinase
TGF-β	transforming growth factor – beta
TIMP-1	tissue inhibitor of metalloproteinase
CTGF	connective tissue growth factor
ALT	alanine aminotransferase
ECM	extracellular matrix
PDGF	platelet derived growth factor
HA	hemagglutinin
DMEM	Dulbecco's modified Eagles medium
FBS	fetal bovine serum
PBS	phosphate buffered saline
MOI	multiplicity of infection
BDL	bile duct ligation
βgal	β-galactosidase

GFP	green fluorescent protein
PI	prodidium iodide
SEM	standard error of the mean
MAKP	mitogen activated protein kinase
PPARγ	peroxisome proliferator activated receptor γ
TBS-T	Tris-buffered saline + Tween-20
mRNA	messenger RNA
RT-PCR	reverse transcription polymerase chain reaction
PCR	polymerase chain reaction
CCl_4	carbon tetrachloride

References

1. Friedman SL. Molecular regulation of hepatic fibrosis, an integrated cellular response to tissue injury. J Biol Chem. 2000; 275:2247–2250. [PubMed: 10644669]
2. Eng FJ, Friedman SL, Fibrogenesis I. New insights into hepatic stellate cell activation: the simple becomes complex. Am J Physiol Gastrointest Liver Physiol. 2000; 279:G7–G11. [PubMed: 10898741]
3. Parker PJ, Waterfield MD. Phosphatidylinositol 3-kinase: a novel effector. Cell Growth Differ. 1992; 3:747–752. [PubMed: 1332743]
4. Reif S, Lang A, Lindquist JN, Yata Y, Gabele E, Scanga A, et al. The role of focal adhesion kinase-phosphatidylinositol 3-kinase-akt signaling in hepatic stellate cell proliferation and type I collagen expression. J Biol Chem. 2003; 278:8083–8090. [PubMed: 12502711]
5. Gentilini A, Marra F, Gentilini P, Pinzani M. Phosphatidylinositol-3 kinase and extracellular signal-regulated kinase mediate the chemotactic and mitogenic effects of insulin-like growth factor-I in human hepatic stellate cells. J Hepatol. 2000; 32:227–234. [PubMed: 10707862]
6. Kim AH, Khursigara G, Sun X, Franke TF, Chao MV. Akt phosphorylates and negatively regulates apoptosis signal-regulating kinase 1. Mol Cell Biol. 2001; 21:893–901. [PubMed: 11154276]
7. Kulik G, Klippel A, Weber MJ. Antiapoptotic signalling by the insulin-like growth factor I receptor, phosphatidylinositol 3-kinase, and Akt. Mol Cell Biol. 1997; 17:1595–1606. [PubMed: 9032287]
8. Coffer PJ, Jin J, Woodgett JR. Protein kinase B (c-Akt): a multifunctional mediator of phosphatidylinositol 3-kinase activation. Biochem J. 1998; 335:1–13. [PubMed: 9742206]
9. Kotani K, Ogawa W, Hino Y, Kitamura T, Ueno H, Sano W, et al. Dominant negative forms of Akt (protein kinase B) and atypical protein kinase Clambda do not prevent insulin inhibition of phosphoenolpyruvate carboxykinase gene transcription. J Biol Chem. 1999; 274:21305–21312. [PubMed: 10409689]
10. Magness ST, Bataller R, Yang L, Brenner DA. A dual reporter gene transgenic mouse demonstrates heterogeneity in hepatic fibrogenic cell populations. Hepatology. 2004; 40:1151–1159. [PubMed: 15389867]
11. Bataller R, Schwabe RF, Choi YH, Yang L, Paik YH, Lindquist J, et al. NADPH oxidase signal transduces angiotensin II in hepatic stellate cells and is critical in hepatic fibrosis. J Clin Invest. 2003; 112:1383–1394. [PubMed: 14597764]
12. Siegmund SV, Uchinami H, Osawa Y, Brenner DA, Schwabe RF. Anandamide induces necrosis in primary hepatic stellate cells. Hepatology. 2005; 41:1085–1095. [PubMed: 15841466]
13. Yata Y, Scanga A, Gillan A, Yang L, Reif S, Breindl M, et al. DNase I-hypersensitive sites enhance alpha1(I) collagen gene expression in hepatic stellate cells. Hepatology. 2003; 37:267–276. [PubMed: 12540776]

14. Uchinami H, Seki E, Brenner DA, D'Armiento J. Loss of MMP 13 attenuates murine hepatic injury and fibrosis during cholestasis. Hepatology. 2006; 44:420–429. [PubMed: 16871591]
15. Isayama F, Hines IN, Kremer M, Milton RJ, Byrd CL, Perry AW, et al. LPS signaling enhances hepatic fibrogenesis caused by experimental cholestasis in mice. Am J Physiol Gastrointest Liver Physiol. 2006; 290:G1318–G1328. [PubMed: 16439470]
16. Parsons CJ, Bradford BU, Pan CQ, Cheung E, Schauer M, Knorr A, et al. Antifibrotic effects of a tissue inhibitor of metalloproteinase-1 antibody on established liver fibrosis in rats. Hepatology. 2004; 40:1106–1115. [PubMed: 15389776]
17. Gäbele E, Reif S, Tsukada S, Bataller R, Yata Y, Morris T, et al. The role of p70S6K in hepatic stellate cell collagen gene expression and cell proliferation. J Biol Chem. 2005; 280:13374–13382. [PubMed: 15677443]
18. Kawada N, Ikeda K, Seki S, Kuroki T. Expression of cyclins D1, D2 and E correlates with proliferation of rat stellate cells in culture. J Hepatol. 1999; 30:1057–1064. [PubMed: 10406184]
19. Jackson LN, Larson SD, Silva SR, Rychahou PG, Chen LA, Qiu S, et al. PI3K/Akt activation is critical for early hepatic regeneration after partial hepatectomy. Am J Physiol Gastrointest Liver Physiol. 2008; 294:G1401–G1410. [PubMed: 18388186]
20. Marra F, Gentilini A, Pinzani M, Choudhury GG, Parola M, Herbst H, et al. Phosphatidylinositol 3-kinase is required for platelet-derived growth factor's actions on hepatic stellate cells. Gastroenterology. 1997; 112:1297–1306. [PubMed: 9098016]
21. Failli P, Ruocco C, De Franco R, Caligiuri A, Gentilini A, Giotti A, et al. The mitogenic effect of platelet-derived growth factor in human hepatic stellate cells requires calcium influx. Am J Physiol. 1995; 269:C1133–C1139. [PubMed: 7491901]
22. Di Sario A, Baroni GS, Bendia E, D'Ambrosio L, Ridolfi F, Marileo JR, et al. Characterization of ion transport mechanisms regulating intracellular pH in hepatic stellate cells. Am J Physiol. 1997; 273:G39–G48. [PubMed: 9252507]
23. Di Sario A, Svegliati Baroni G, Bendia E, Ridolfi F, Saccomanno S, Ugili L, et al. Intracellular pH regulation and Na+/H+ exchange activity in human hepatic stellate cells: effect of platelet-derived growth factor, insulin-like growth factor 1 and insulin. J Hepatol. 2001; 34:378–385. [PubMed: 11322198]
24. Monick MM, Powers LS, Barrett CW, Hinde S, Ashare A, Groskreutz DJ, et al. Constitutive ERK MAPK activity regulates macrophage ATP production and mitochondrial integrity. J Immunol. 2008; 180:7485–7496. [PubMed: 18490749]
25. del Peso L, Gonzalez-Garcia M, Page C, Herrera R, Nunez G. Interleukin-3-induced phosphorylation of BAD through the protein kinase Akt. Science. 1997; 278:687–689. [PubMed: 9381178]
26. Galli A, Crabb DW, Ceni E, Salzano R, Mello T, Svegliati-Baroni G, et al. Antidiabetic thiazolidinediones inhibit collagen synthesis and hepatic stellate cell activation *in vivo* and *in vitro*. Gastroenterology. 2002; 122:1924–1940. [PubMed: 12055599]
27. Miyahara T, Schrum L, Rippe R, Xiong S, Yee HF Jr, Motomura K, et al. Peroxisome proliferator-activated receptors and hepatic stellate cell activation. J Biol Chem. 2000; 275:35715–35722. [PubMed: 10969082]
28. Hazra S, Xiong S, Wang J, Rippe RA, Krishna V, Chatterjee K, et al. Peroxisome proliferator-activated receptor gamma induces a phenotypic switch from activated to quiescent hepatic stellate cells. J Biol Chem. 2004; 279:11392–11401. [PubMed: 14702344]
29. Yavrom S, Chen L, Xiong S, Wang J, Rippe RA, Tsukamoto H. Peroxisome proliferator-activated receptor gamma suppresses proximal alpha1(I) collagen promoter via inhibition of p300-facilitated NF-I binding to DNA in hepatic stellate cells. J Biol Chem. 2005; 280:40650–40659. [PubMed: 16216869]
30. Kisseleva T, Uchinami H, Feirt N, Quintana-Bustamante O, Segovia JC, Schwabe RF, et al. Bone marrow-derived fibrocytes participate in pathogenesis of liver fibrosis. J Hepatol. 2006; 45:429–438. [PubMed: 16846660]

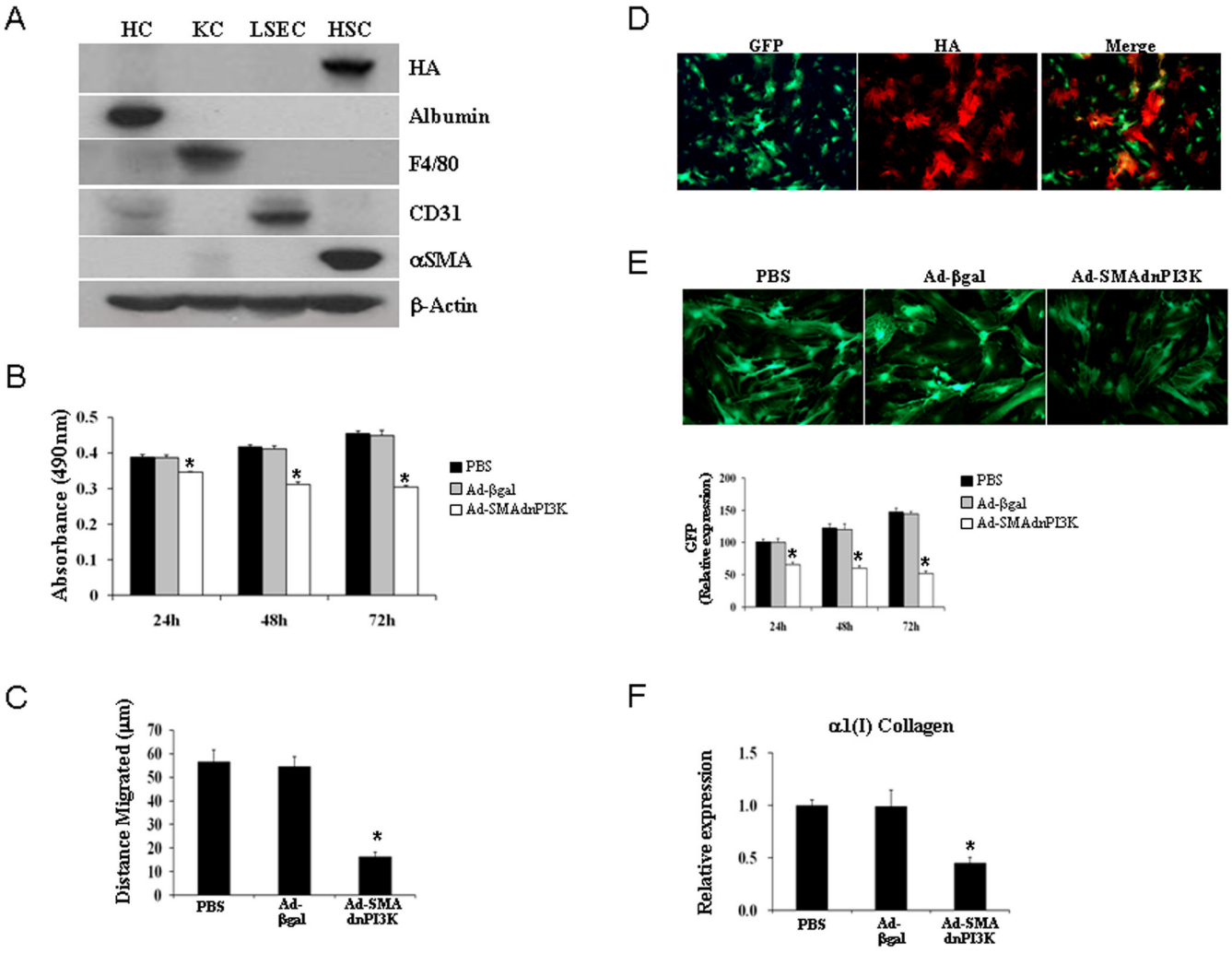

Figure 1. Inhibition of PI3K signaling with Ad-SMAdnPI3K reduces HSC proliferation, migration, and collagen gene expression

(A) Each cell was cultured in proper medium containing 10% FBS for 5 days and was transduced at a MOI of 300 with Ad-SMAdnPI3K. After 48 hr of incubation, whole cell extracts were prepared for Western blots of HA, albumin, F4/80, CD31, αSMA and β-actin. HC: hepatocyte, KC: Kupffer cell, LSEC: liver sinusoidal endothelial cell, HSC: hepatic stellate cell. Results are representative of 3 independent experiments. **(B)** Culture-activated HSCs were treated with PBS or transduced with Ad-βgal or Ad-dnSMAPI3K and cell proliferation assessed after 24 hr, 48 hr, and 72 hr following stimulation with 10% FCS. P = 0.0007, P = 0.0006, P = 0.0006, respectively, compared to Ad-βgal. **(C)** Cell migration, using a wound assay, was assessed in culture-activated HSCs treated with PBS in cells transduced with Ad-βgal or Ad-SMAdnPI3K after 24 hr. P = 0.0008 compared to Ad-βgal. **(D)** Co-localization of GFP (green) and HA (red) expression in HSCs isolated from pCol9GFP-HS4,5 transgenic mice transduced with Ad-SMAdnPI3K. **(E)** GFP expression, assessed by fluorescence microscopy, in HSCs isolated from pCol9GFP-HS4,5 mice 2 days following Ad-SMAdnPI3K transduction. Original magnification, ×100 with quantification of GFP fluorescence using phosphorimager analysis, in culture-activated HSCs 24 hr, 48 hr, and 72 hr following PBS treatment or transduction of pCol9GFP-HS4,5 HSCs with either Ad-βgal or Ad-SMAdnPI3K. Original magnification ×200. **(F)** Steady state levels of α1(I)

collagen mRNA was determined by quantitative real-time RT-PCR. Data are expressed as the mean ± SEM from 3 independent experiments. *P<0.01 *vs*. Ad-βgal transduced cells.

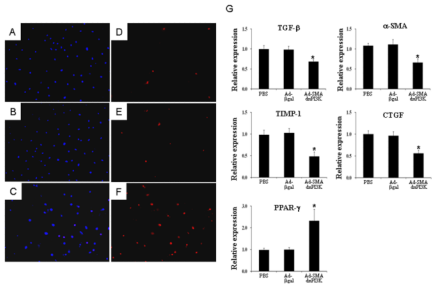

Figure 2. Transduction of Ad-SMAdnPI3K induces cell death in activated HSCs and reduces profibrotic gene expression

Hoechst 33342 **(A – C)** and propidium iodide (PI) **(D – F)** staining in culture-activated (Day 5) pCol9GFP,HS4,5 HSCs. **(A, D)** control cells, **(B, E)** cells transduced with Ad-βgal; **(C, F)** cells transduced with Ad-SMAdnPI3K. After 24h cells were incubated with Hoechst (1 μg/ml) and PI (5 μg/ml) for 20 min. Figures are representative data from three independent experiments. Original magnification ×100. **(G)** Culture activated (Day 5) HSCs from pCol9GFP-HS4,5 mice were transduced with Ad-SMAdnPI3K, Ad-βgal, or no virus and incubated for 48 hr. Steady state mRNA levels for TGF-β, αSMA, TIMP-1, CTGF, and PPAR-γ were quantified by RT-PCR. Data are expressed as the mean ± SEM from 3 independent experiments. **P*<0.05 *vs*. Ad-βgal transduced cells.

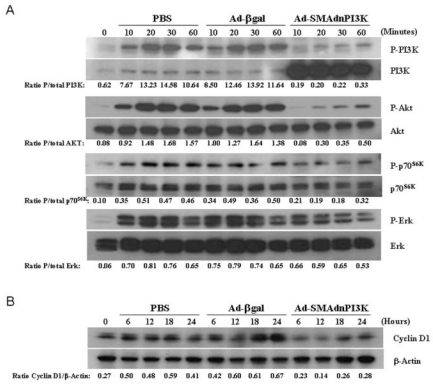

Figure 3. Inhibition of PI3K activity blocks the activation of PI3K/Akt/p70^{S6K} signaling and reduces cyclin D1 expression

(A, B) HSCs from pCol9GFP-HS4,5 were cultured for 5 days and then transduced with indicated adenoviruses. Cells were serum starved for 48 hr, then stimulated with 10% FBS. Whole cell extracts were prepared at the indicated time points and Western blots for P-PI3K, PI3K, P-Akt, Akt, P-p70^{S6K}, P-ERK, ERK, cyclin D1, and β-actin performed. Results are representative of 3 independent experiments.

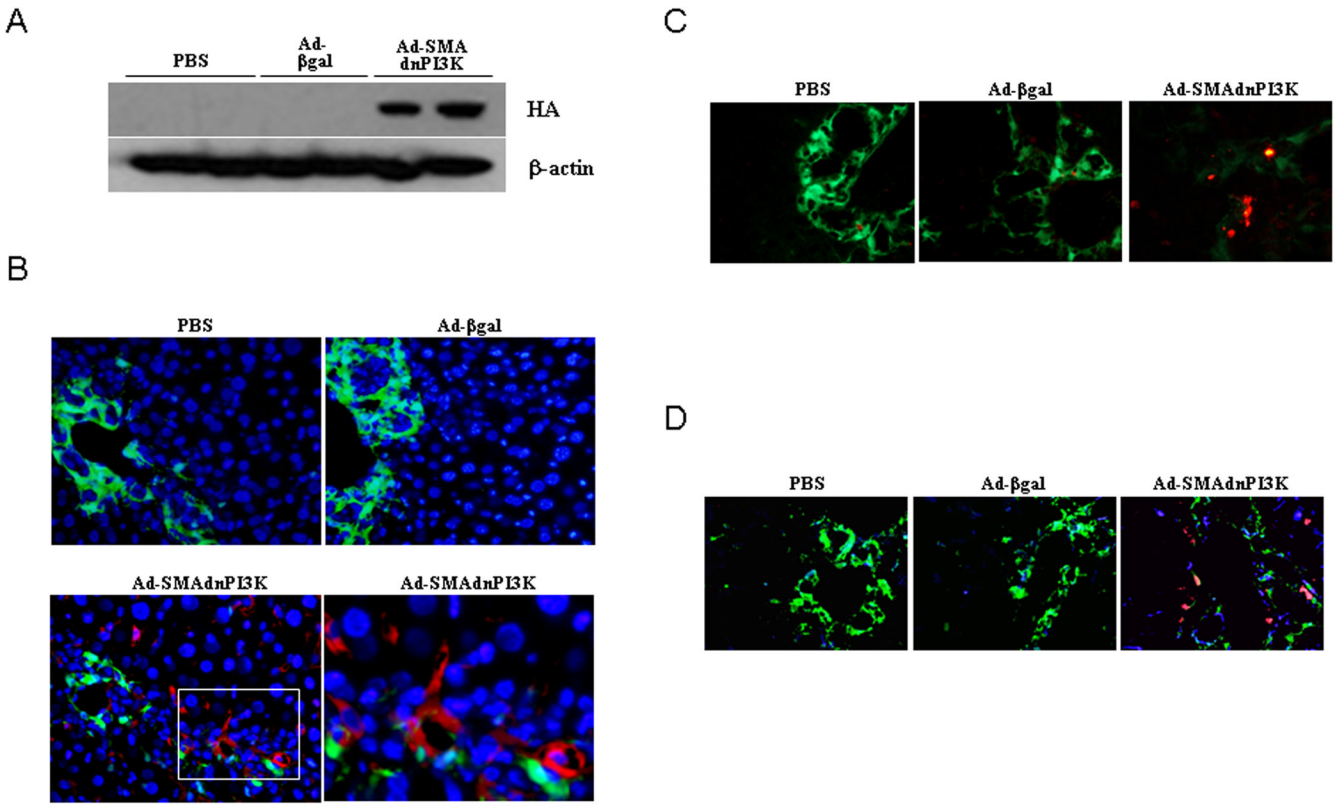

Figure 4. Ad-SMAdnPI3K expresses the HA-tag in the liver and induces apoptosis in fibrotic liver

(A) BDLs were performed on Day 0, and adenovirus administered on Day 4. Proteins were collected from whole liver 2 days after adenoviral administration. HA-tag expression was detected in the liver extracts by Western Blot analysis. **(B)** HA expression was assessed 2 days after adenoviral administration by immunofluorescent staining using a monoclonal HA antibody (Red). Original magnification, ×200. **(C)** Liver cell death was assessed on Day 9 after BDL TUNEL (Day 5 after adenoviral transduction) in liver tissue. Original magnification, ×200. **(D)** Immunofluorescence staining shows localization of collagen (green), desmin (blue) and HA (red) 2 days after adenoviral administration. Original magnification, ×200. n = 6 animals per group.

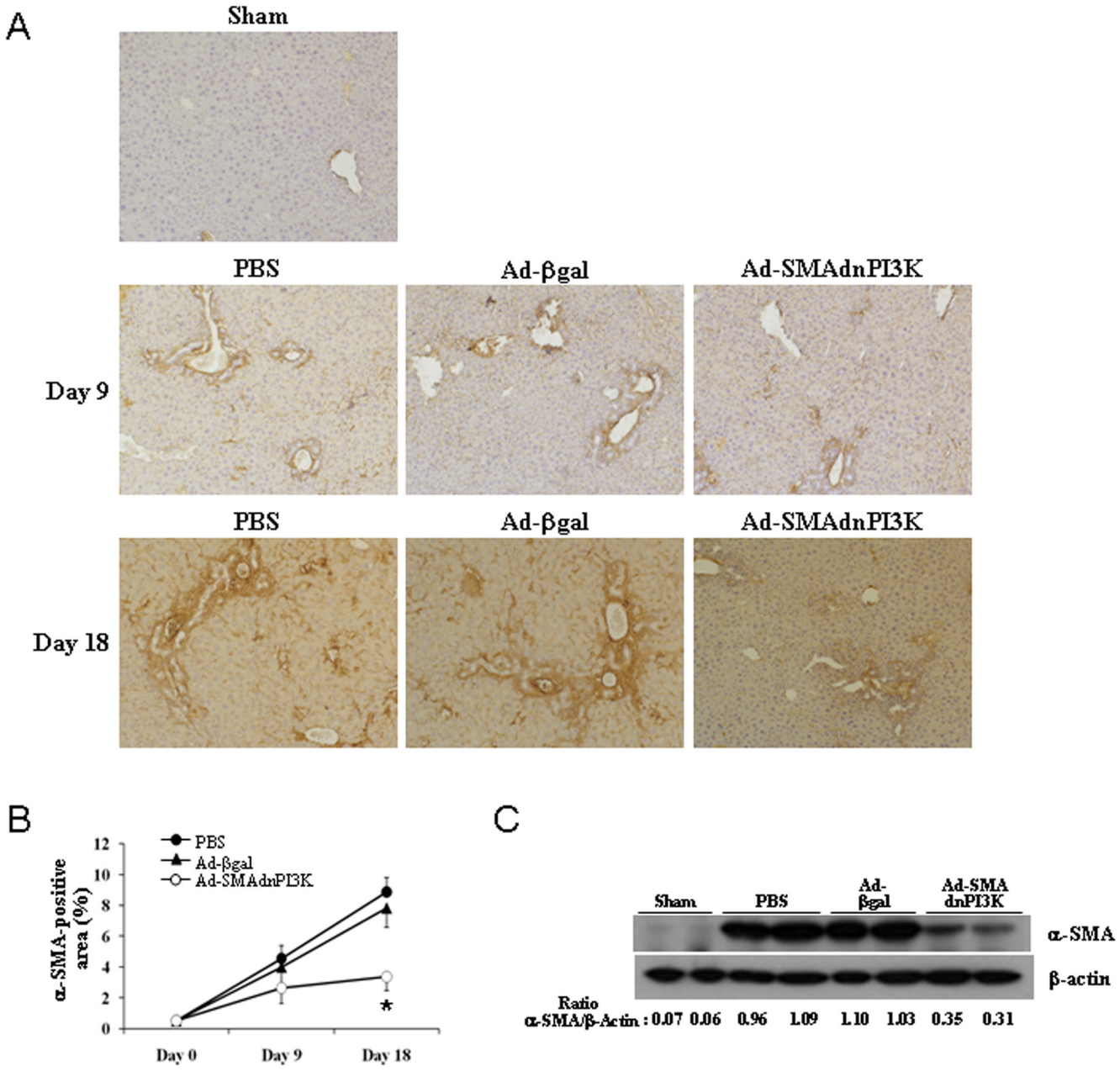

Figure 5. Transduction of Ad-SMAdnPI3K inhibits αSMA expression in BDL-treated mice

(A) αSMA expression was examined in paraffin-embedded liver tissue of pCol9GFP-HS4,5 mice 9 days after BDL (5 days after adenoviral transduction) and 18 days after BDL (14 days after adenoviral transduction) stained using an αSMA antibody. Original magnification, ×100. **(B)** Quantification of αSMA stained area. **(C)** Western blot analysis for αSMA expression 18 days after BDL (14 days after adenoviral transduction). n= 6 animals per group.

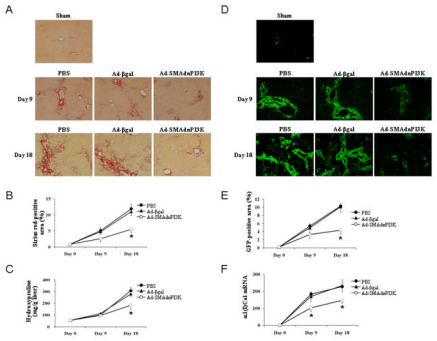

Figure 6. Administration of Ad-SMAdnPI3K attenuates liver fibrosis in BDL-treated mice

(A) Paraffin-embedded tissue of pCol9GFP-HS4,5 mice 9 days after BDL (5 days after adenoviral transduction) and 18 days after BDL (14 days after adenoviral transduction) were stained with Sirius red. Original magnification, ×100. **(B)** Quantification of Sirius red stained area. **(C)** Quantitation of hepatic hydroxyproline content. **(D)** GFP expression in pCol9GFP-HS4,5 mice after 9 days and 18 days following BDL (5 days and 14 days, respectively, after adenoviral transduction) visualized by fluorescent microscopy. Sham tissue was examined at Day 9. Original magnifications, Day 18 ×40, Sham and BDL Day 9 ×100. **(E)** Percentage of GFP positive area, in ×100 fields, was quantified using the NIH Image J software. **(F)** Steady state α1(I) collagen mRNA levels at Day 18 after BDL (n = 6 animals per group). **P*<0.05 *vs*. Ad-βgal treated mice.

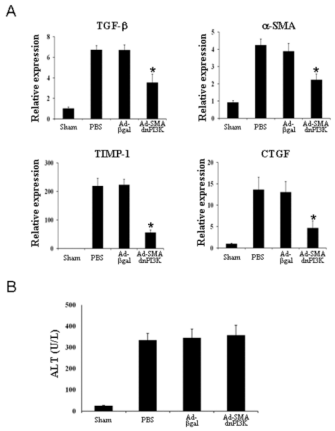

Figure 7. Administration of Ad-SMAdnPI3K inhibits profibrotic gene expression in the livers of BDL-treated mice, but does not affect ALT levels

(A) Steady state mRNA levels of TGF-β, αSMA, TIMP-1, and CTGF 9 days after BDL (Day 5 after adenoviral transduction) as determined by quantitative real-time RT-PCR. Data are presented as mean ± SEM from 6 anmials per group **P*<0.05 *vs*. animals administered Ad-βgal. **(B)** Serum ALT levels 9 days after BDL (Day 5 after adenoviral transduction; n = 6 animals per group).